

## **SUPPLEMENTARY MATERIALS**

**Fig. S1. Loss of p38 $\alpha$  signaling does not enhance TPA-induced skin inflammation.**

**Fig. S2. The refractoriness of epidermal side population cells to dye labeling depends on verapamil-sensitive membrane transporters.**

**Fig. S3. Loss of p38 $\alpha$  signaling does not reduce p63 mRNA amounts in epidermal keratinocytes and epidermal-derived tumors.**

**Fig. S4. p63 mRNA and protein amounts vary in different types of human cancer and among different human cancer cell lines.**

**Fig. S5. p38 $\alpha$  phosphorylates p63 in vitro.**

**Fig. S6. p38 $\alpha$  is required for inducing or attenuating specific target genes in keratinocytes.**

**Fig. S7. p63 represses MMP13 expression in keratinocytes.**

**Table S1. LC-MS/MS detection of  $\Delta$ Np63 $\alpha$ -derived phosphopeptides containing p38 phosphoacceptor sites.**

**Table S2. Oligonucleotide primers used in real-time qPCR.**

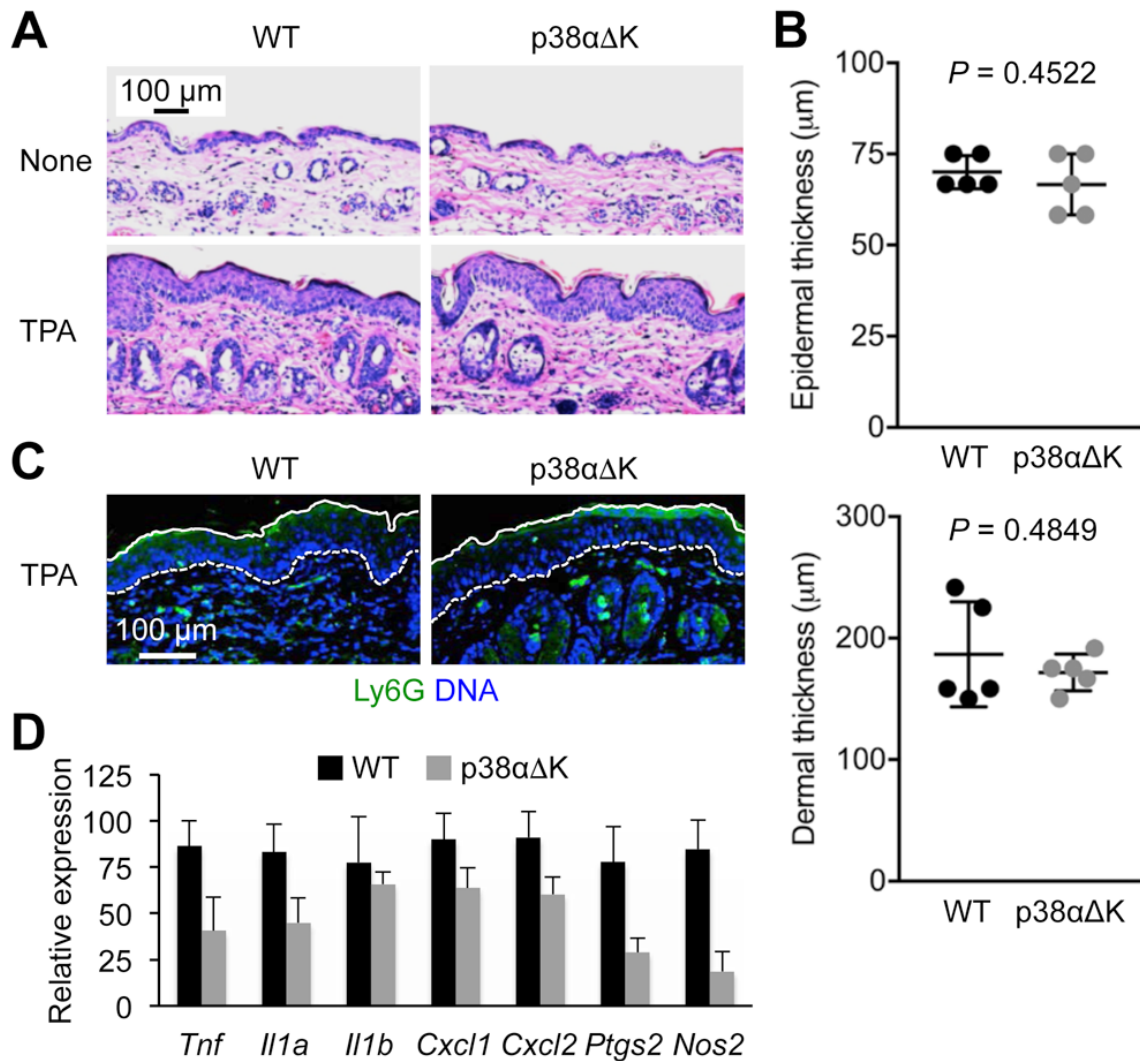


**Fig. S1. Loss of p38α signaling does not enhance TPA-induced skin inflammation.**

(A-D) Mice (n = 5 per group) were left unprovoked (None) or subjected to TPA-induced skin inflammation. Skin sections were analyzed by H&E staining (A). Epidermal and dermal thickness in TPA-treated mice was determined from H&E-stained skin images and are shown as means ± SD (B). *P* values by two-tailed unpaired Student's *t* test (B). Skin sections were analyzed by immunostaining/counterstaining for the indicated molecules (C). Solid and dotted line, epidermal margins and the epidermal-dermal boundary, respectively (C). Images are representative of five tissue sections. TPA-treated skin was subjected to RNA isolation and qPCR analysis (D). qPCR data are means ± SD of four biological replicates.

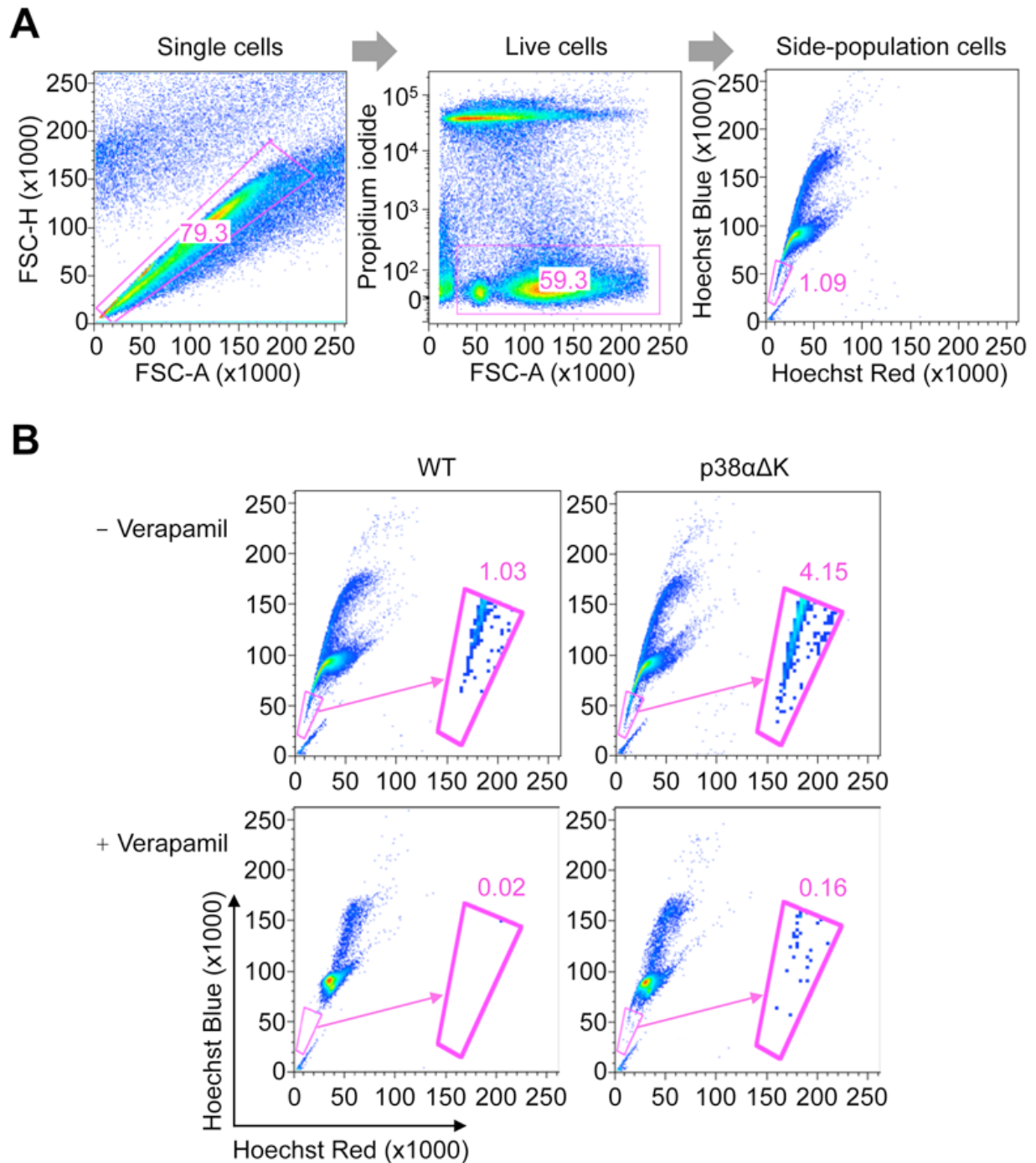


**Fig. S2. The refractoriness of epidermal side population cells to dye labeling depends on verapamil-sensitive membrane transporters.**

(A and B) Steady-state mouse epidermal cells were incubated with Hoechst33342 and analyzed by flow cytometry as in Fig. 4C. The gating strategy used for detecting side populations is shown (A). Cells were preincubated with verapamil or not as indicated before Hoechst33342 exposure and flow cytometry (B). Data are representative of three experiments.

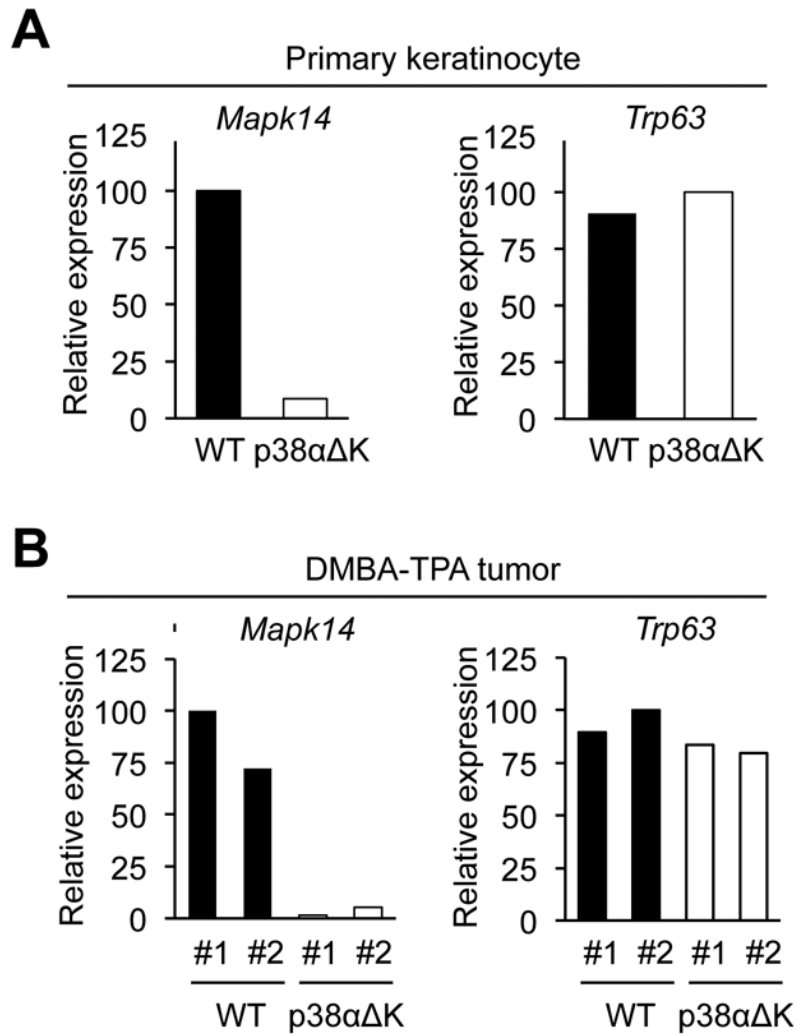


**Fig. S3. Loss of p38 $\alpha$  signaling does not reduce p63 mRNA amounts in epidermal keratinocytes and epidermal-derived tumors.**

(A and B) Epidermal keratinocytes and DMBA-TPA-induced tumors (#1 and #2) from mice were subjected to RNA isolation and qPCR analysis. Data are representative of three experiments.

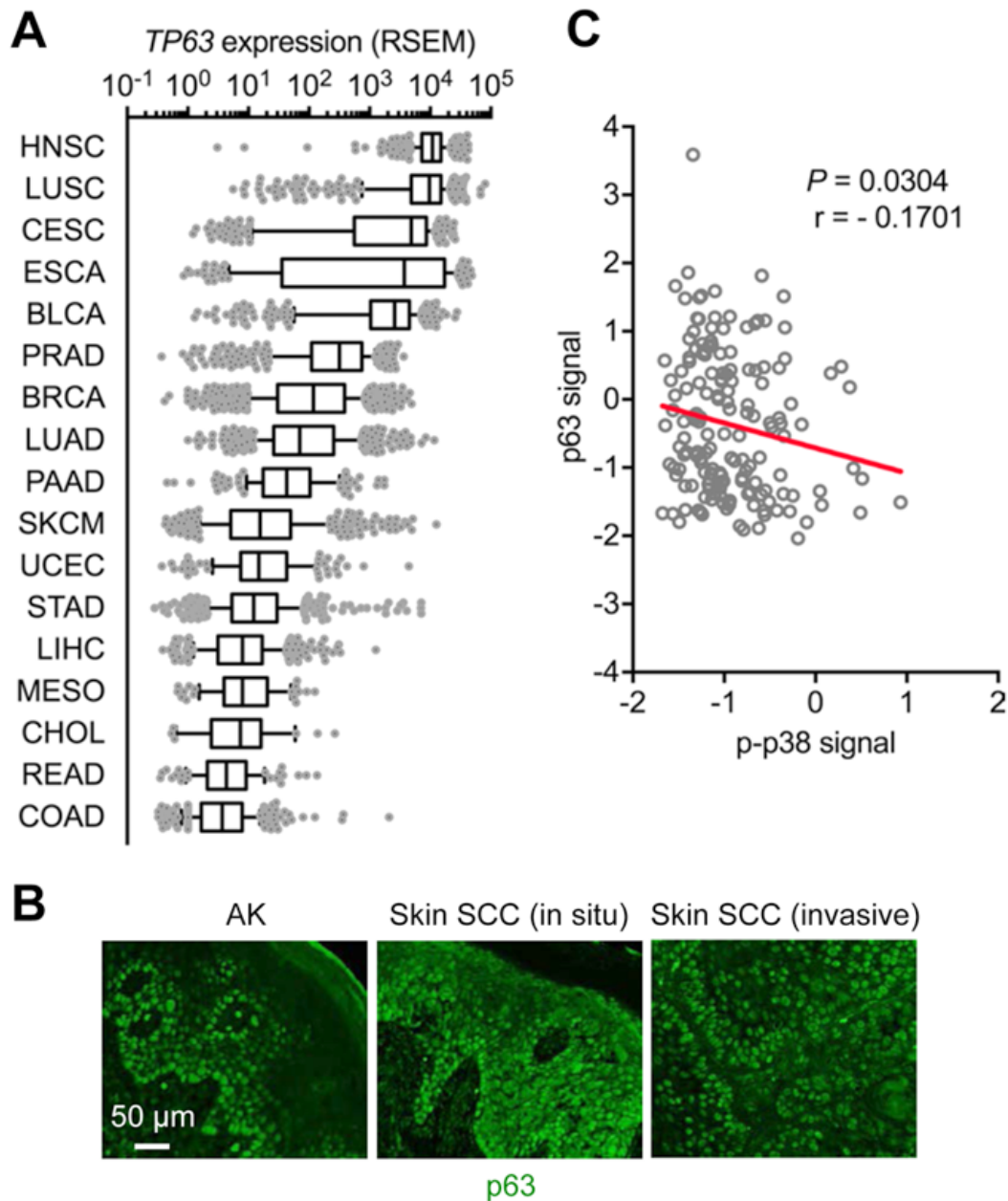


**Fig. S4. p63 mRNA and protein amounts vary in different types of human cancer and among different human cancer cell lines.**

(A) p63 mRNA amounts in human tumors were analyzed using the TCGA RNA-Seq dataset.

(B) Human AK skin and skin SCC tumor sections were analyzed by immunostaining for p63.

(C) p63 protein amounts and phosphorylated p38 signals in human cancer cell lines were analyzed using the RPPA dataset of the MD Anderson Cell Lines Project. p-, phosphorylated. Images are representative of five tissue sections.

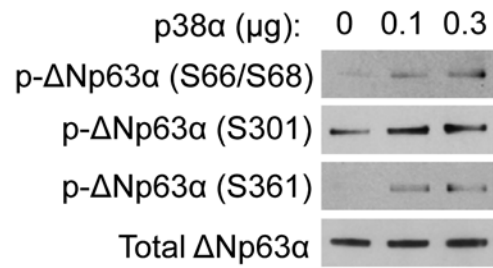


**Fig. S5. p38 $\alpha$  phosphorylates p63 in vitro.**

Recombinant p63 protein was phosphorylated with recombinant p38 $\alpha$  in kinase reactions and analyzed by immunoblotting. Blots are representative of three experiments.

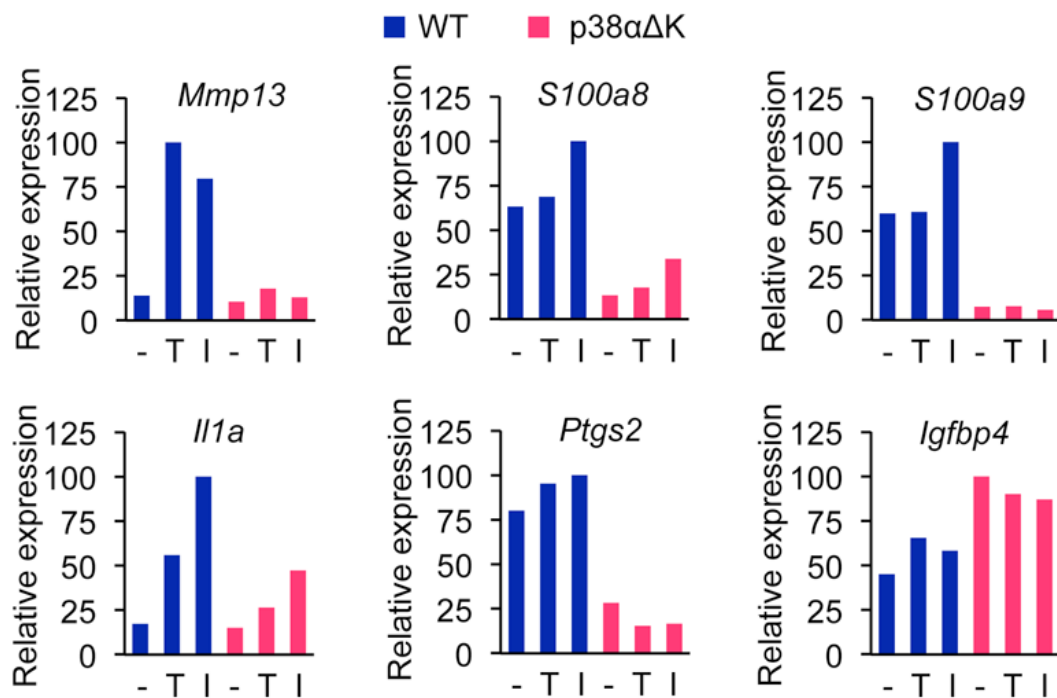


**Fig. S6. p38 $\alpha$  is required for inducing or attenuating specific target genes in keratinocytes.** Mouse Keratinocytes were left unstimulated or stimulated with TPA (T; 100 nM) and interleukin-1 (I; 20 ng/ml). RNA prepared 4 hours after stimulation was analyzed by qPCR. Data are representative of three experiments.

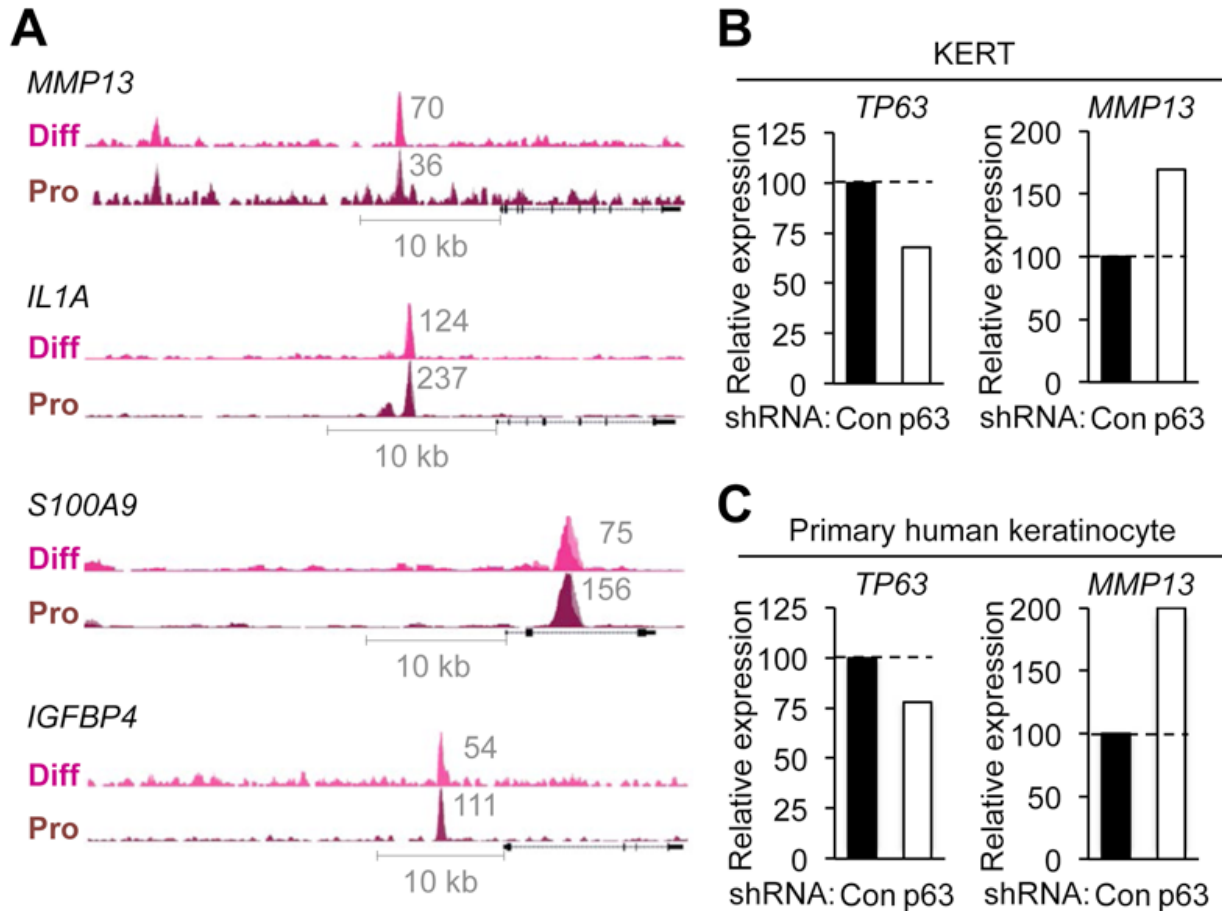


**Fig. S7. p63 represses MMP13 expression in keratinocytes.**

(A) ChIP-Seq data showing p63 occupancy in differentiated (Diff) and proliferating (Pro) human keratinocytes (Gene Expression Omnibus GSE59827) were visualized as custom tracks on the UCSC genome browser. Numbers beside peaks indicate normalized peak heights (proportional to the relative amounts of chromatin-bound p63).

(B and C) RNA from KERT cells (B) and human keratinocytes (C) infected with control (Con) or p63 shRNA-expressing lentiviruses was analyzed by qPCR. Data are representative of three experiments.



**Table S1. LC-MS/MS detection of  $\Delta$ Np63 $\alpha$ -derived phosphopeptides containing p38 phosphoacceptor sites.**

Phosphoacceptor or residue	Phosphopeptides from 293T cells expressing p38 $\alpha$ <sup>CA</sup>	Phosphopeptides from in vitro kinase reactions
Thr123	VM <b>p</b> TPPPQGAVIR	VM <b>p</b> TPPPQGAVIR
Ser301	<b>p</b> SPDDELLYLPVR RR <b>p</b> SPDDELLYLPVR	
Ser361	QTSIQ <b>p</b> SPSSYGNS <b>p</b> SPPLNK	QTSIQ <b>p</b> SPSSYGNS <b>p</b> SPPLNK QKQTSIQ <b>p</b> SPSSY
Ser369	QTSIQSPSSYGNS <b>p</b> SPPLNK QTSIQ <b>p</b> SPSSYGNS <b>p</b> SPPLNK	

**Table S2. Oligonucleotide primers used in real-time qPCR.**

Gene	Forward primer (5' to 3')	Reverse primer (5' to 3')
<i>Cxcl1</i>	gccaatgagctgcgctgt	ccttcaagctctggatgttcttg
<i>Cxcl2</i>	atccagagcttgagtgtgacgc	aaggcaaacttttgaccgcc
<i>Igfbp4</i>	cttcatcatccccattccaa	cactgtttggggtggaagt
<i>Il1a</i>	tccagggcagagagggagt	ggaactttggccatcttgatt
<i>Il1b</i>	gtggctgtggagaagctgtg	gaaggtccacgggaaagacac
<i>Mapk14</i>	gcatcgtgtggcagttaaga	gtcctttggcgtgaatgat
<i>Mmp13</i>	tttattgttctgcccata	ggccttgagtgatccaga
<i>Nos2</i>	caagcaccttgaagaggag	ccaatgtgcttgcaccac
<i>Ppia</i>	atggtcaaccccaccgtgt	ttcttgctgtctttggaactttgc
<i>Ptgs2</i>	ccccacagtcaaagacact	ggttctcagggatgtgagga
<i>S100a8</i>	gagttccttgcgatggtgat	tggtgtcttttgatgatgc
<i>S100a9</i>	accaccatcatcgacacctt	tgtcagggtgtccttccttc
<i>Tnf</i>	acagaaagcatgatccgcg	gcccccatcttttggg
<i>Trp63</i>	acagggcattgtctcttctg	ccacaacacaactgcattcc
<i>GAPDH</i>	cgtggaaggactcatgacca	gccatcacgccacagtttc
<i>MMP13</i>	tggtccaggagatgaagacc	atttgtctggcgtttttgga
<i>TP63</i>	ccagcttatcaaccctcagc	tgccatcaggaatggttgta